Engineering Transactions, **73**(3): 421–440, 2025, https://doi.org/10.24423/engtrans.3490.2025
Institute of Fundamental Technological Research Polish Academy of Sciences (IPPT PAN)
Université de Lorraine • Poznan University of Technology

SiMRTRANS

Energy Efficiency of an LPG-Powered Extended-Range Electric Vehicle

Paweł KRAWCZYK, Artur KOPCZYŃSKI*, Jakub LASOCKI

Faculty of Automotive and Construction Machinery Engineering
Warsaw University of Technology
Warsaw, Poland; e-mails: pawel.krawczyk@pw.edu.pl, jakub.lasocki@pw.edu.pl

*Corresponding Author e-mail: artur.kopczynski@pw.edu.pl

This paper deals with energy efficiency evaluation of an extended range electric vehicle (EREV) equipped with a range extender (REX) powered by liquefied petroleum gas (LPG). The investigation is based on simulation, with key input data derived from empirical studies carried out by the authors. It includes four target driving ranges (200, 300, 400, 500 km), six driving cycles (WLTC 3b, FTP-75, CLTC-P, Artemis 130, NYCC, HWFET) and three battery size variants for the WLTC 3b cycle. The influence of the these factors on the overall efficiency and specific energy consumption of the EREV is assessed. The results are analyzed in terms of the number of REX activations per 100 km and the total REX operating time.

Keywords: extended-range electric vehicle; efficiency; energy consumption; LPG.

Notations

Abbreviations

BAT	–	battery pack,
BEV	–	battery electric vehicle,
BSFC	–	brake specific fuel consumption,
CLTC-P	–	China light-duty vehicle test cycle,
CS	–	control strategy,
DC	–	driving cycle,
ECU	–	electronic control unit,
EM	–	electric motor,
EMS	–	energy management system,
EREV	–	extended-range electric vehicle,
EV	–	electric vehicle,
FT	–	fuel tank,
FTP	–	federal test procedure,

G – electric generator,
HEV – hybrid electric vehicle,
ICE – internal combustion engine,
LPG – liquefied petroleum gas,
NYCC – New York City cycle,
PMSM – permanent magnet synchronous motor,
PS – power summing node,
REX – range extender,
SOC – state of charge,
VE – vehicle and driveline,
W – road wheels,
WLTC – worldwide harmonized light-Duty test cycle.

Symbols and parameters

$\mathrm{BSFC}_{\mathrm{LPG}}$ – REX LPG brake specific fuel consumption [g/kWh],
E_{bat} – used battery energy [kWh],
E_{ch} – energy spent for battery charging [kWh],
E_d – energy spent for driving [kWh],
E_{LPG} – energy from used LPG [kWh],
$F_d(t)$ – momentary total resistance force [N],
n_{on} – number of REX starts during the drive [–],
P_b – battery power at its terminals [W],
P_g – REX power at its terminals [W],
P_m – electric machine power at its terminals [W],
t – time [s],
$v(t)$ – momentary vehicle speed [m/s],
V_{LPG} – volume of used LPG [dm^3],
$V_{\mathrm{LPG}on}$ – volume of LPG used during single REX start [dm^3],
η – vehicle efficiency [%],
η_{cb} – converter efficiency: battery to power summing node [%],
η_{cg} – converter efficiency: REX to power summing node [%],
η_{ch} – charger efficiency [%],
η_{cm} – converter efficiency: EM terminals to power summing node [%],
ρ_{LPG} – LPG density [$\mathrm{kg/dm}^3$].

1. Introduction

An EREV is a type of electric vehicle (EV) in which propulsion is provided solely by an EM, but which also includes a relatively small internal combustion engine (ICE) that generates extra electric energy to recharge the battery when needed [1]. Alternatively, some researchers consider such a system as series hybrid with significantly larger batteries, due to the similarity in their components and operating principles [2]. A major factor driving the development of EREVs is the need to increase the driving range of conventional battery electric vehicles (BEVs). This is accomplished in such a way that

once the vehicle battery reaches a certain level of discharge or is unable to provide the instantaneous power required to meet vehicle demand, the ICE is activated to power a generator, which either recharges the battery or directly provides electricity to the EM. This setup helps overcome the fundamental range limitations of BEVs [2, 3] while still provides the ability to operate EREVs in fully electric mode over short distances, making them as environmentally friendly as BEVs.

The benefits of EREVs go beyond extended driving range and the ability to operate solely on electric power. One significant advantage is the high overall energy efficiency of the system. This is possible because the ICE is not mechanically connected to the vehicle's wheels. As a result, it avoids operating under dynamic conditions associated with frequent acceleration and deceleration in typical road traffic. In contrast to traditional ICE-driven systems, where fuel consumption increases due to the dynamic nature of driving [4], the ICE in an EREV operates in a stationary mode at certain selected operating points that are optimized in terms of power output and fuel consumption. The result is a high level of energy efficiency for the entire system. This topic has been extensively investigated, with findings well documented in the literature [5, 6].

Current research on EREVs focuses on further improving efficiency, which can be achieved by developing an appropriate drive system control strategies to be implemented in the vehicle energy management system (EMS). Numerous scientific works have been published in this field. For example, Lan *et al.* [7] explored – using both experiments and simulations – how driving pattern, power management strategy and additional power sources affect vehicle fuel efficiency. A real-time optimized EMS was proposed in [8], aiming to enhance system efficiency and battery lifespan [9]. Additionally, a real-time hardware platform was created to test the suggested method's feasibility. Another study [10] developed an EMS using deep reinforcement learning for hybrid battery configurations in EVs. The findings confirmed the proposed strategy's effectiveness. Du *et al.* [11] worked on a power management strategy for EREVs with varying battery capacities to enhance energy efficiency. Paper [12] applied a dynamic programming approach to optimize energy management, considering both battery health and range extender fuel consumption. Paper [13] developed a range extender model validated by experimental data and suggested an energy management optimization strategy for power allocation. The CS for EREV was also a subject of research conducted by the authors of the current paper, with example publications including [14, 15].

Considerably less research has been carried out on another potential solution to enhancing EREVs performance: supplying the ICE with alternative fuels. Di Ilio *et al.* [16] developed a model for a hydrogen-powered rotary engine to assess its suitability as a REV for compact hybrid vehicles with ultra-low emis-

sions. Paper [17] presents a methanol-hydrogen engine system based on a Miller cycle methanol engine designed for applications in EREV. Paper [18] considers an EREV equipped with a combined cycle gas turbine, which offers not only high efficiency but also multi-fuel capability. Finally, the authors of the current paper have focused on developing the EREV concept using an ICE fuelled by liquefied petroleum gas(LPG), investigating various aspects if this approach [19, 20]. LPG offers significant potential to reduce the emission of harmful substances from ICEs and represents a cost-effective alternative to current range extension technologies, which predominantly utilize gasoline [21]. Moreover, compared to other alternative fuels, LPG has a relatively high calorific value of about 104.5 MJ/m^3 in gaseous form and about 45.6 MJ/kg in liquid form (data for a mixture of 50% propane and 50% butane) [22]. In contrast, other gaseous alternative fuels have lower calorific values, e.g., hydrogen at 10.77 MJ/m^3, methane at 35.82 MJ/m^3, and biogas (mainly methane) at approx. 24.2 MJ/m^3 [22]. A significant advantage of LPG is its well-established distribution infrastructure, with widespread availability for automotive use in many countries, including Italy, Poland, Turkey, and other countries.

The aim of this paper is to evaluate the energy efficiency of an EREV equipped with an LPG-fuelled ICE. The investigation is based on modeling, using key input data derived from empirical studies carried out by the authors. Details of the model, as well as the proposed EMS CS, are presented. The analysis takes into account several scenarios with different assumptions regarding DCs, driving range and vehicle battery size.

2. Materials and methods

2.1. Powertrain

The vehicle powertrain is configured as a series hybrid electric vehicle (HEV) with a range extender (REX), as depicted in Fig. 1. The layout includes an electric motor (EM), a battery pack (BAT), an electronic control unit (ECU), and

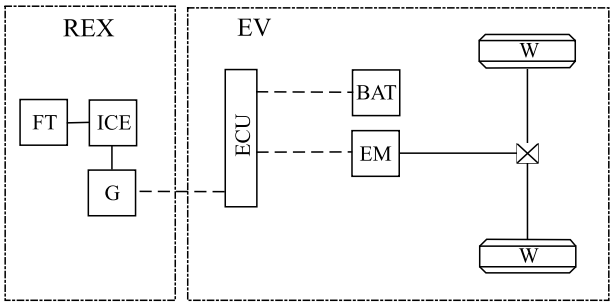

Fig. 1. Diagram of the vehicle powertrain.

road wheels (W). Additionally, an LPG-powered ICE coupled with an electric generator (G) and a fuel tank (FT) provides extended driving range. In an EREV configuration, a larger battery and a smaller generator are employed, combined with a dedicated CS. The detailed structure and operating principles of this configuration are described in [15, 20].

2.2. Simulation model

2.2.1. Topology of the model with simulation inputs and outputs. Figure 2 presents the overall topology of the simulation model. It integrates various components, including the vehicle and driveline (VE), the EM, the BAT, the REX, and a central power summing node (PS), all coordinated by a control strategy (CS). The primary simulation inputs are the DC and the required travel distance, while the main outputs include total travelled distance, fuel consumption, and battery state of charge (SOC). Multiple DCs (Fig. 3) and required travel distances (200, 300, 400, and 500 km) are considered as simulation inputs. For detailed information on modeling procedures, parameter selection, and validation procedures, refer to [14, 15, 20].

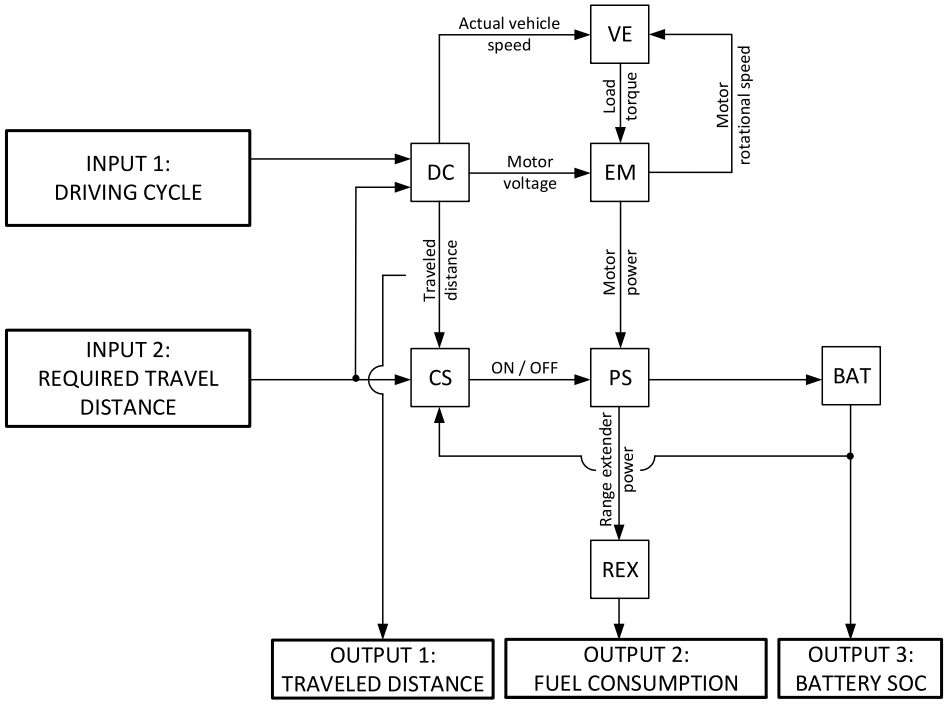

Fig. 2. Topology of the simulation model. The diagram features: VE – vehicle driveline, EM – electric motor, DC – driving cycle, PS – power summing node, CS – control strategy, BAT – battery, and REX – range extender.

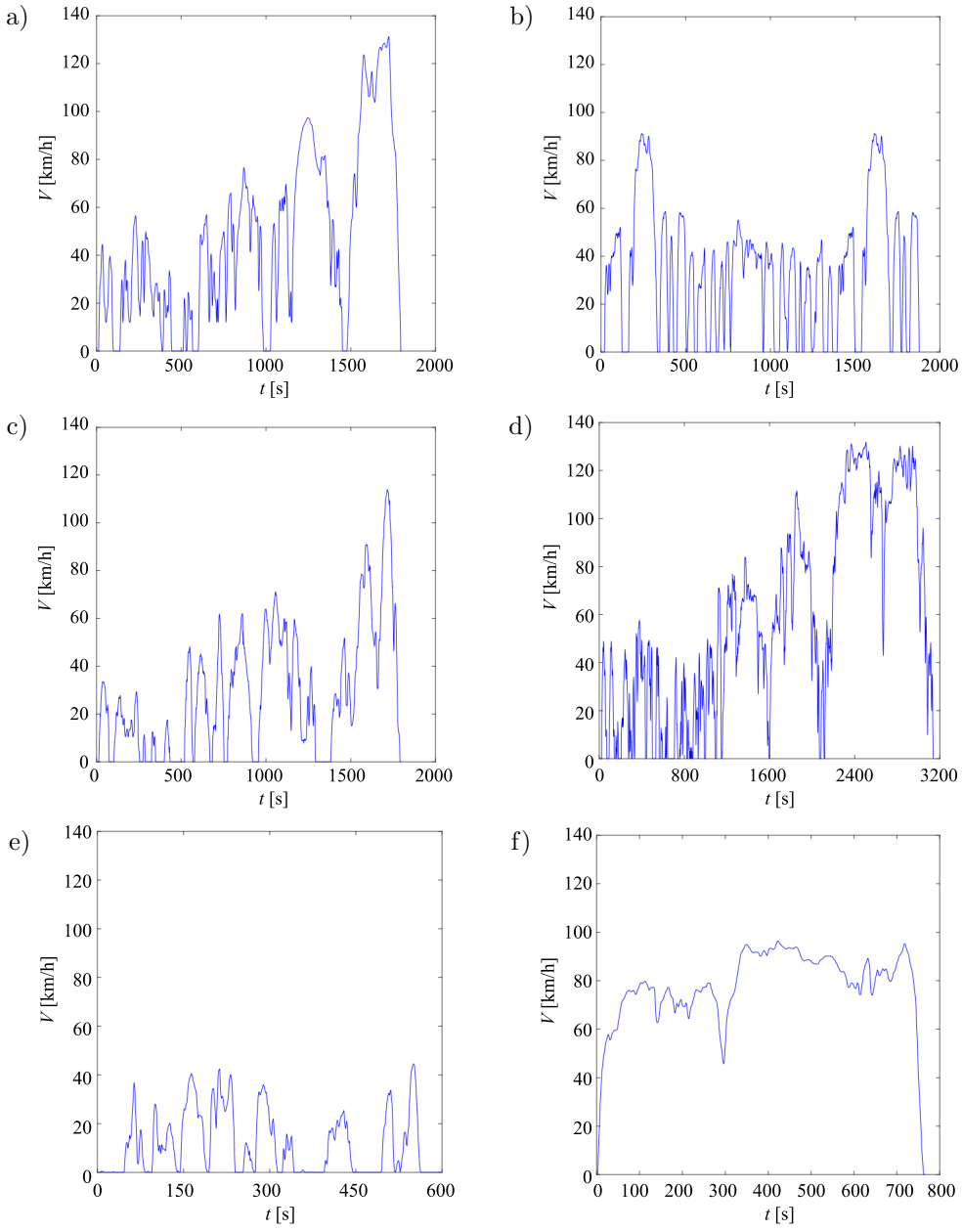

FIG. 3. Speed profiles over time for the DCs included in the study: a) WLTC 3b, b) FTP-75, c) CLTC-P, d) Artemis 130, e) New York City Cycle (NYCC), and f) HWFET.

2.2.2. Model of the REX with PS. The LPG-powered REX is integrated into the system to supplement electrical energy and extend the vehicle's driving range. Its operating maps (e.g., BSFC and efficiency characteristics), along with

the scaling approach and control activation logic, are fully described in [14, 15, 20]. The PS serves as an idealized junction that manages instantaneous power distribution between the EM, BAT, and REX. This node ensures that the power demand imposed by the DC is met while accounting for energy conversion efficiencies and the selected CS. Power distributions obey Eq. (2.1) and the schematic representation is depicted in Fig. 4.

$$P_m \eta_{cm}^{\operatorname{sign}(P_m)} + P_{mb} \eta_{cb}^{\operatorname{sign}(P_b)} + P_g \eta_{cg} = 0, \tag{2.1}$$

where P_m – EM power at its terminals [W], P_b – BAT power at its terminals [W], P_g – REX power at its terminals [W], η_{cm} – converter efficiency for energy transfer between EM terminals, PS, η_{cb} – converter efficiency for energy transfer between battery terminals and PS, and η_{cg} – converter efficiency for energy transfer between REX terminals and PS.

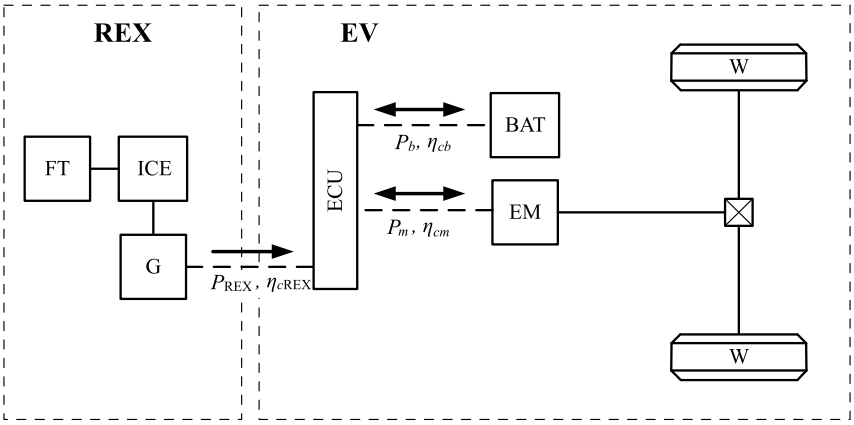

FIG. 4. Illustration of power flow between the EM, BAT, and REX through the PS.

Figure 4 provides a schematic overview of the PS' multiple operations, with specific power flow cases outlined in Table 1.

TABLE 1. Power flow scenarios between the EM, BAT, and REX, based on in Eq. (2.1). Source power is positive, and receiver power is negative.

Case	Motor power P_m	Battery power P_b	REX power P_g
EV only – driving	$P_m < 0$	$P_b > 0$	$P_g = 0$
EV only – braking	$P_m > 0$	$P_b < 0$	$P_g = 0$
REX on – driving, $-P_m > \eta_{cg}\eta_{cm}P_g$	$P_m < 0$	$P_b > 0$	$P_g > 0$
REX on – driving, $-P_m < \eta_{cg}\eta_{cm}P_g$	$P_m < 0$	$P_b < 0$	$P_g > 0$
REX on – braking	$P_m > 0$	$P_b < 0$	$P_g > 0$

The CS is designed to ensure that the target travel distance is reached at a predefined SOC level. By adjusting REX operation and battery usage, the vehicle adheres to the required driving profile. The summation of power at the PS is a key element of the model. Under various operating conditions – including pure EV mode, braking with regenerative energy flow, and engine-assisted driving – instantaneous power contributions from each component are combined with the PS node.

2.2.3. Set parameters values for the test object model. Some relevant vehicle parameters, such as gear ratios, specifications, battery characteristics, and REX performance characteristics – are based on previously validated experimental and simulation datasets, described comprehensively in [14, 15, 20]. These includes lithium-ion cell parameters, PMSM ratings, and the BSFC maps for the REX. Drag coefficient, frontal area and traction wheels parameters are modeled based on Toyota Yaris Cross (Tables 2 and 3).

Table 2. Vehicle simulation parameters.

Parameter	Test mass	Frontal drag coefficient	Frontal area	Gear ratios	Drivetrain efficiency
Value	1741	0.35	2.39	13.2/6.6	94
Unit	kg	–	m^2	–	%

Table 3. Traction wheel specifications.

Parameter	Single wheel inertia	Tire rolling resistance coefficient	Tire dynamic radius
Value	1.065	0.0084	0.326
Unit	$kg \cdot m^2$	–	m

The PS' efficiency values (η_{cg}, η_{cm}, and η_{cb}) are each set at 96%, with a 500 W auxiliary load representing the average power consumption of vehicle support system. The BSFC map and selected operating point of the REX are shown in Fig. 5, with corresponding parameters in Table 4.

Table 4. Selected REX operating point parameters for simulation.

Parameter	Output power	Rotation speed	Engine torque	BSFC (LPG)
Value	16.6	2400	66	269.9
Unit	kW	rpm	$N \cdot m$	g/kWh

The BSFC of the generator can be converted to its efficiency. The efficiency map and the selected operating point of the REX running on LPG are shown in Fig. 6.

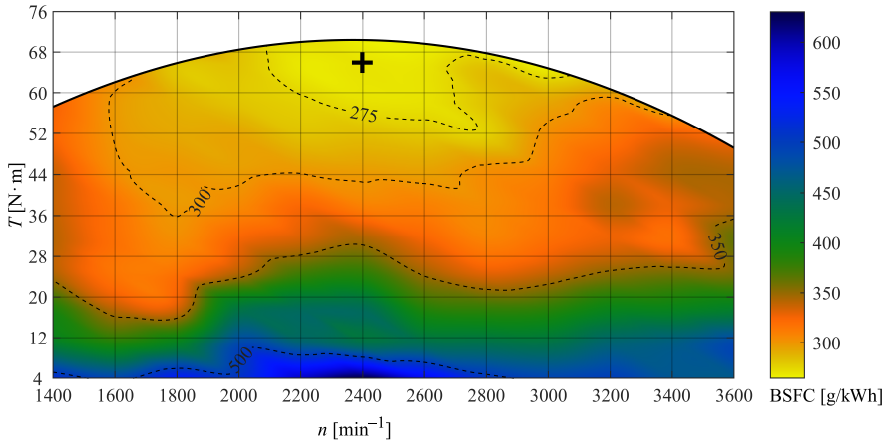

FIG. 5. BSFC map and the selected operating point of the REX running on LPG [20].

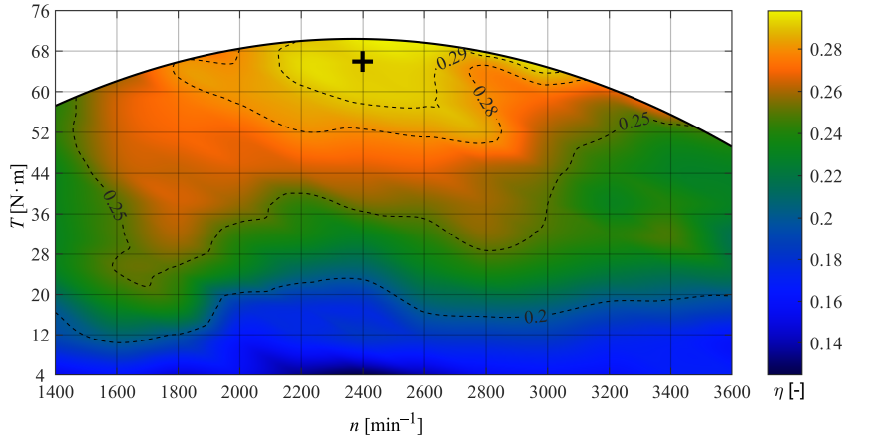

FIG. 6. Efficiency map and operating point of the REX running on LPG [20].

The efficiency of the vehicle in EV mode is given by Eq. (2.2):

$$\eta = \frac{E_d}{E_{ch}}, \tag{2.2}$$

where E_d – energy spent for driving [kWh] (see Eq. (2.3)), and E_{ch} – energy spent for battery charging [kWh] (see Eq. (2.4)),

$$E_d = \frac{\int F_d(t) \cdot v(t)\ \mathrm{d}t}{3.6 \cdot 10^6}, \tag{2.3}$$

where $F_d(t)$ – momentary total resistance force [N], and $v(t)$ – momentary vehicle speed [m/s], the energy spent for battery charging is:

$$E_{ch} = \frac{E_{\text{bat}}}{\eta_{ch}}, \tag{2.4}$$

where $\eta_{ch} = 0.9$ – charger efficiency, E_{bat} – used battery energy [kWh].

The efficiency of the vehicle in REX mode is given by Eq. (2.5):

$$\eta = \frac{E_d}{E_{ch} + E_{\text{LPG}}}, \tag{2.5}$$

where E_{LPG} – energy of the LPG fuel used [kWh] is calculated as:

$$E_{\text{LPG}} = (V_{\text{LPG}} + n_{on} \cdot V_{\text{LPG}on}) \cdot \rho_{\text{LPG}} \cdot \frac{\text{BSFC}_{\text{LPG}}}{1000}, \tag{2.6}$$

where V_{LPG} – volume of LPG used [dm^3], n_{on} – number of REX starts during the drive, $V_{\text{LPG}on} = 0.01$ dm^3 – volume of LPG used during a single REX start, $\rho_{\text{LPG}} = 0.549$ kg/dm^3 – density of LPG, and $\text{BSFC}_{\text{LPG}} = 269.6$ g/kWh – BSFC of the LPG-powered REX.

2.3. Conditions for simulation testing

To ensure that the simulation produces practical and repeatable results, a set of constraints is incorporated. The following assumptions define the test conditions:

- The vehicle strictly follows the given speed profiles.
- Vehicle mass remains constant during the simulated drive.
- Environmental effects (wind, rain, atmospheric pressure, and temperature) are ignored.
- No road gradient is considered. The road is assumed to be flat.
- Fuel parameters for REX remain constant.
- No startup delay for the REX.
- Speed control is uniform across all DCs.
- Thermal effects on the motor, controller, and battery are neglected, assuming sufficient cooling.
- The motor never operates beyond its specified torque and speed limits.
- Gear changes are instantaneous.
- There is no loss of tire-to-road traction during simulation.

The model was built in MATLAB-Simulink® and simulated using the ODE45 (Runge–Kutta) solver with a fixed time step of 0.01 s and tolerances set at $1 \cdot 10^{-7}$. The model can calculate performance metrics such as CO_2eq emissions under various REX scenarios, fuel consumption, driving range, and battery energy use per 100 km. In this paper, however, the focus is on powertrain efficiency and specific energy consumption. The battery SOC is assumed to be charged from 0.15 to 0.9 before the trip.

3. Results and discussion

Figure 7 shows the simulation results for the overall efficiency of the vehicle's powertrain operating under six different DCs: WLTC 3b, Artemis 130, FTP-75, NYCC, CLTC-P, and HWFET. Data points corresponding to the same DC were approximated by a double exponential function to facilitate the interpretation of trends. The results shown in the graph include BEV, marked with green circles, and the EREV mode with ICE assistance, evaluated for four target driving ranges: 200 km, 300 km, 400 km, and 500 km. The vehicle was equipped with a 23.8 kWh primary battery.

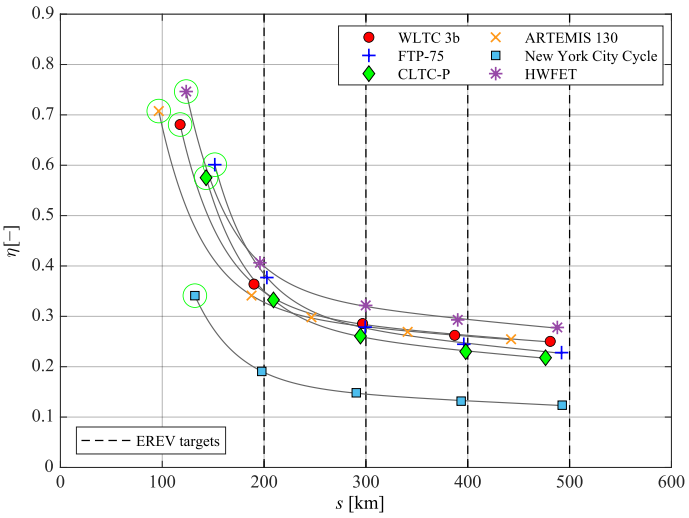

Fig. 7. Overall efficiency of the vehicle powertrain in BEV mode (points highlighted with green circles) and EREV mode for different DCs and target ranges of 200 km, 300 km, 400 km, and 500 km.

As expected, the efficiency of the drive system was the highest for driving in pure electric mode. Specifically, efficiency values obtained ranged from 34% in the NYCC to 75% in the HWFET. Excluding the lowest result, this efficiency range can be significantly narrowed to 60–75%. The distance traveled by the vehicle in pure electric driving mode ranged from 96.6 km in the Artemis 130 cycle up to about 151.6 km in the FTP-75 cycle.

In the driving mode with the REX activated, the vehicle's efficiency decreased significantly. There was a clear downward trend as the target range increase, reflecting the CS' settings. In general, for a 200 km target range, efficiency was 19–41%, for 300 km 15–32%, for 400 km 13–29%, and for 500 km 12–29%, with the highest efficiency consistently recorded in the HWFET cycle, while the NYCC cycle consistently showed the lowest efficiency. Excluding

the NYCC cycle, the efficiency differences between cycles were generally within 20% of the best result. The decline in the drive system's efficiency in EREV mode stems from the need to supplement the additional required energy to charge the battery from the REX, which operates at low efficiency, even at its optimal point characterized by minimal specific fuel consumption.

The above results draw attention to the issue of the influence of driving patterns on the efficiency of the EREVs. This is a well-known phenomenon and applies to almost every type of vehicle, especially those powered solely by ICE. Each DC differs in its dynamic properties, which are determined by the speed profile (Fig. 3). Not only the average and maximum speeds are important here, but also the intensity of acceleration and braking, as well as the frequency and duration of stops. Analyzing it from the perspective of the EREV powertrain, each DC subjects the electric traction motor to a different set of operating states characterized by different torque and rotational speeds. Moreover, the potential for recovering braking energy varies between cycles. In the case of the NYCC, which simulates urban driving with traffic congestion, the operating states of the electric traction motor are forced to operate predominantly at low efficiency (in low-torque and low rotational speed), with low potential for recovering energy from braking. In this particular scenario, the motor operates in a low-speed regime for an extended period. Because its ability to generate adequate electromotive force is limited at low speeds, producing sufficient braking torque requires higher electrical currents, which in turn increase electrical losses. Consequently, losses are higher than in other cycles, reducing regenerative braking efficiency. As the motor's rotational speed decreases, it can only recover kinetic energy when the braking power exceeds the sum of mechanical and electrical losses. Overall, this leads to higher energy consumption per unit of distance traveled.

Figure 8 shows the specific energy consumption of the vehicle powertrain, expressed in kWh/100 km. The results in the graph refer to the same simulation variants as discussed earlier for efficiency: pure electric driving (BEV mode), driving with REX assistance (EREV mode), four target driving ranges and six DCs. The data points corresponding to the same DC are approximated by a double exponential function. The vehicle was equipped with a 23.8 kWh primary battery.

Specific energy consumption is a typical criterion value for comparing different BEVs. In this simulation, the vehicle in pure electric mode achieved results ranging from about 13 kWh/100 km in the FTP-75 cycle to about 21 kWh/100 km in the Artemis 130 cycle. The results of the latter clearly stand out against the results of the other cycles, in which the specific energy consumption did not exceed 17 kWh/100 km.

For the drive system operation in EREV mode, supported by LPG fuel combustion in the engine, the specific energy consumption is much higher. As ex-

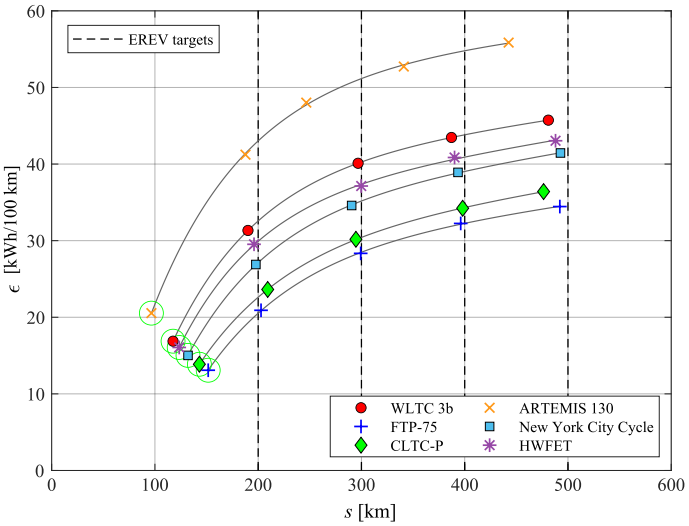

FIG. 8. Specific energy consumption of the vehicle powertrain in BEV mode (points highlighted with green circles) and EREV mode for different DCs and target ranges of 200 km, 300 km, 400 km, and 500 km.

pected, an inverse relationship is observed compared to efficiency, i.e., specific energy consumption increases with the increasing target range. The greater the distance the vehicle must travel in EREV mode, the more the battery is supplemented by the REX, which consumes LPG fuel. As a result, for a range of 200 km, specific energy consumption ranged from about 21 to 41 kWh/100 km, for 300 km – 28–48 kWh/100 km, for 400 km – 32–53 kWh/100 km, and for 500 km – 34–56 kWh/100 km. Similar to the BEV mode, the results with the lowest specific energy consumption corresponded to the FTP-75 cycle, while the highest was for the Artemis 130 cycle.

The trends described above can be explained by analyzing the frequency of REX operation across different DCs. Figure 9 shows the number of REX activations per 100 km of traveled distance. These are results for the least favorable variant, with a target range of 500 km. Figures 10 and 11 show histograms depicting the distribution of REX activations relative to their operating duration per activation, for target ranges of 200 km and 500 km, respectively.

The highest number of REX activations per 100 km, almost 14, occurred in the NYCC cycle, which certainly reduced the overall efficiency of the powertrain. It is important to mention that during the NYCC cycle, the REX operation was usually short – for the target range of 500 km, most activations lasted between 2 and 4 minutes. This results from the vehicle speed profile typical of urban driving in this DC, in which the vehicle moves at low speeds and accelerates and brakes frequently.

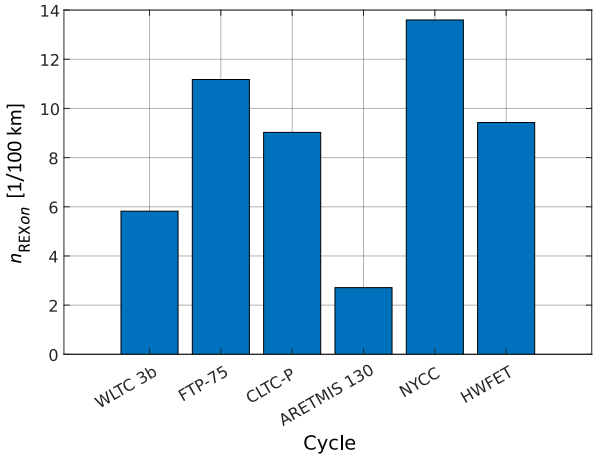

FIG. 9. Number of REX activations per 100 km of distance traveled by the vehicle for each DC.

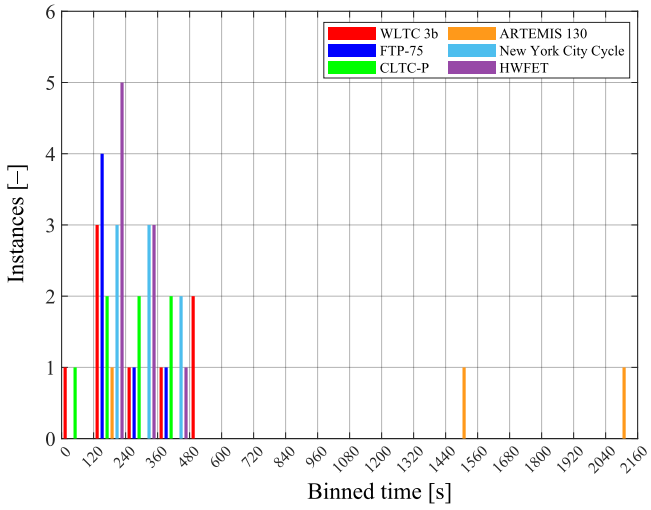

FIG. 10. Histogram of the number of REX activations versus operating time per activation for a target range of 200 km.

Non-obvious results were obtained for the Artemis 130 cycle. In this cycle, the REX was activated the least often, on average less than 3 times per 100 km. This could potentially indicate the highest efficiency and lowest specific energy consumption. However, the actual results differed. While the efficiency of the drive system in this cycle was not the highest, it was comparable the other cycles, but the specific energy consumption was significantly higher. The explanation lies in the histogram of REX activations versus time. It can be seen that in the case of this cycle, REX was activated rarely, but they lasted for exceptionally long time. For a target range of 500 km, one of the activations lasted

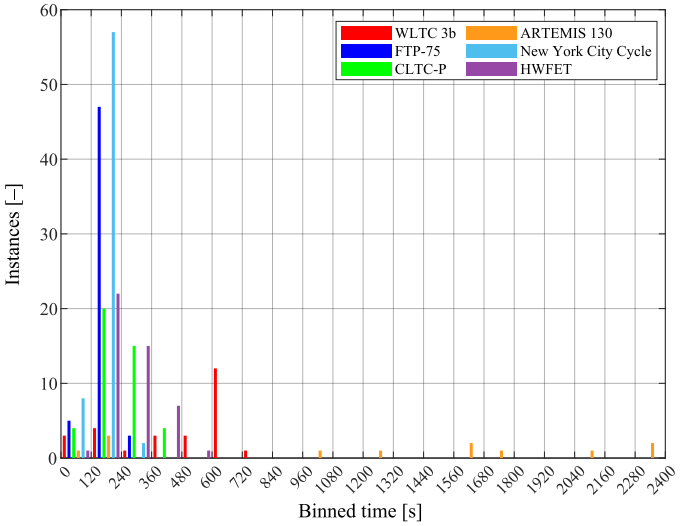

FIG. 11. Histogram of the number of REX activations versus operating time per activation for a target range of 500 km.

nearly 40 min. No other cycle showed such behavior, so the cause must be related to the speed profile of the Artemis 130 cycle. Indeed, this cycle includes urban, rural and motorway segments. The latter is particularly energy-intensive, lasting about 18 min, which is more than one-third of the entire cycle time, and the vehicle covers a distance of almost 29 km, which is 56% of the total distance of this cycle.

Generally, the duration of a single REX activation has significant implications in the context of specific fuel consumption and overall powertrain efficiency. Intuitively, shorter ICE operation times reduce fuel consumption, thus improving the overall efficiency of an EREV. However, frequent short ICE activations, in large numbers per unit of distance traveled, result in the so-called "fuel consumption penalty", caused by the additional fuel needed to start the ICE repeatedly. This leads to a deterioration of overall efficiency of the powertrain. Nevertheless, it is necessary to distinguish between REX activation in order to recharge the battery or providing a temporary power boost to the electric part of the powertrain, and continuous ICE operation for a several dozen minutes. The latter case significantly increases fuel consumption and reduces the efficiency of EREV.

Additional simulations were performed for two variants of the vehicle battery capacity: one 50% larger and the other 50% smaller than the baseline. The overall efficiency and specific energy consumption for these variants are shown in Figs. 12 and 13, respectively. For better readability, these results are limited to the WLTC DC only.

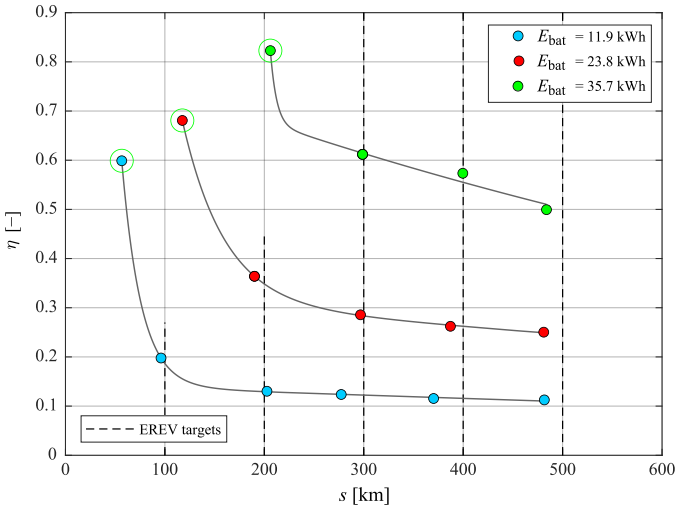

FIG. 12. Impact of battery capacity on the overall efficiency of the vehicle powertrain in BEV mode (points highlighted with green circles) and in EREV mode, operating under the WLTC cycle with target ranges of 200 km, 300 km, 400 km, and 500 km.

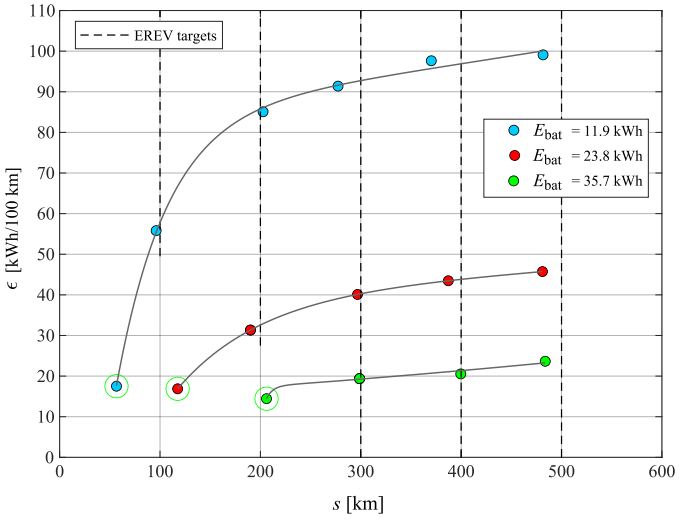

FIG. 13. Impact of battery capacity on the specific energy consumption the vehicle powertrain in BEV mode (points highlighted with green circles) and in EREV mode, operating under the WLTC cycle with target ranges of 200 km, 300 km, 400 km, and 500 km.

It is clearly visible that increasing the battery capacity by 50% has a positive effect on both the overall efficiency and specific energy consumption, despite the associated increase in vehicle weight. In pure electric mode (BEV), efficiency increased slightly by 21%, while in ICE-assisted mode (EREV), this difference reached a maximum of 119% (for the target range of 400 km). A similar trend can

be observed for specific energy consumption. In the case of BEV mode, the savings reached 14%, while in EREV mode the reduction was as much as 53% (for the target range of 400 km). These improvements are associated with an increase in the share of driving with a purely electric power supply, which is by definition characterized by greater efficiency. As a result of the larger battery capacity, the purely electric range of the vehicle increased from 117.5 km to 206.1 km.

On the other hand, reducing the battery capacity by 50% clearly degrades the vehicle's performance compared to a vehicle with a standard battery. Overall efficiency in BEV mode decreased by 12%, while in EREV mode it dropped by up to 64% (for the range of 200 km). Specific energy consumption in BEV mode increased by only 4% but in EREV mode it surged by as much as 172% (also for the range of 200 km). The main reason is the significant reduction in the pure electric range, from 117.5 km to 56.6 km, which significantly increases the share of ICE-assisted driving compared to the model with standard battery.

When interpreting the results for different battery capacities, it should be emphasized that the applied powertrain CS [15] was optimized for the standard battery. While this has minimal effect on the increased battery capacity variant, it significantly affects the performance of the reduced battery capacity model. This is manifested, among other things, in the vehicle's inability to reach the intended target ranges above 200 km. This also occurs for variants with standard and increased battery capacity, but not to such a large extent.

When discussing the vehicle's ability to achieve the assumed target ranges in EREV mode (200 km, 300 km, 400 km, and 500 km), it should be emphasized that the applied powertrain CS [15], threats the target range as a hypothetical value – it indicates approximately the point at which the battery SOC will stop at a value of 15%, which is a fairly conservative and safe assumption. In reality, if the vehicle were to continue driving beyond this point, it would reach the target range at SOC of about 12–13%.

4. Conclusions

This study investigated the EREV efficiency under real-world driving conditions, represented by the WLTC 3b, FTP-75, CLTC-P, ARTEMIS 130, NYCC and HWFET. The analysis was carried out based on the simulation performed in MATLAB-Simulink®. It included four different target driving ranges (200, 300, 400, and 500 km), alongside three variants of battery size specifically tested for WLTC 3b drive. The EREV model, based on component modeling, incorporated an LPG REX and BEV configuration, enabling calculations of vehicle efficiency and specific fuel consumption. From the results obtained, the following conclusions can be drawn:

- The EREV powertrain efficiency ranged from 12.36 to 40.64% for cases with a 23.8 kWh battery. While these values are respectable, they fall short of the BEV mode efficiency range of 34.11–74.64%.
- EREV powertrain specific energy consumption spanned from 20.91 to 55.86 kWh/100 km for the 23.8 kWh battery variants. Therefore EREV mode uses significantly more energy than the BEV mode range of 13.08–20.54 kWh/100 km.
- Increasing the size of the battery in the EREV improves powertrain efficiency.
- The frequency and duration of REX activations strongly depend on the selected target driving range and parameters of the driving cycle.

The conducted EREV efficiency simulation tests indicate the significant influence of DC parameters, battery size, and both the duration and frequency of REX activations on the overall efficiency of the powertrain. Even minor modifications to the CS may result in variations in powertrain performance.

Future research could focus on a detailed analysis of how specific driving patterns (DCs) affect fuel consumption and overall efficiency of EREVs. Driving conditions, as expressed through speed profiles of driving patterns, can be quantified using time- or distance-averaged parameters. Another potential research direction would be to compare the results presented in this paper with those obtained for other powertrain control strategies. After all, it is the chosen strategy that plays a decisive role in shaping the characteristics and performance of EREVs [15].

Author contributions

All authors significantly contributed to this research. All authors have reviewed and accepted the final published version of the manuscript.

Funding

This research received no external funding.

Data availability statement

All relevant data are presented in the paper and in the authors' previously published works cited in the references.

Acknowledgments

The authors would like to acknowledge the infrastructural support provided by the Institute of Vehicles and Construction Machinery Engineering, Faculty

of Automotive and Construction Machinery Engineering, Warsaw University of Technology, Warsaw, Poland.

Conflicts of interest

The authors declare that there are no known competing financial interests or personal relationships that could have influenced the work reported in this paper.

References

1. Wang Y., Biswas A., Rodriguez R., Keshavarz-Motamed Z., Emadi A., Hybrid electric vehicle specific engines: State-of-the-art review, *Energy Reports*, **8**: 832–851, 2022, https://doi.org/10.1016/j.egyr.2021.11.265.
2. Lakshmi Prasad S., Gudipalli A., Range-anxiety reduction strategies for extended-range electric vehicle, *International Transactions on Electrical Energy Systems*, **2023**: 7246414, 2023, https://doi.org/10.1155/2023/7246414.
3. Rainieri G., Buizza C., Ghilardi A., The psychological, human factors and socio-technical contribution: A systematic review towards range anxiety of battery electric vehicles' drivers, *Transportation Research Part F: Traffic Psychology and Behaviour*, **99**: 52–70, 2023, https://doi.org/10.1016/j.trf.2023.10.001.
4. Chłopek Z., Biedrzycki Z., Lasocki J., Wójcik P., Assessment of the impact of dynamic states of an internal combustion engine on its operational properties, *Eksploatacja i Niezawodność – Maintenance and Reliability*, **17**(1): 35–41, 2015, https://doi.org/10.17531/ein.2015.1.5.
5. Puma-Benavides D.S., Izquierdo-Reyes J., Calderon-Najera J.d.D., Ramirez--Mendoza R.A., A systematic review of technologies, control methods, and optimization for extended-range electric vehicles, *Applied Sciences*, **11**(15): 7095, 2021, https://doi.org/10.3390/app11157095.
6. Tran M.-K., Bhatti A., Vrolyk R., Wong D., Panchal S., Fowler M., Fraser R., A review of range extenders in battery electric vehicles: Current progress and future perspectives, *World Electric Vehicle Journal*, **12**(2): 54, 2021, https://doi.org/10.3390/wevj12020054.
7. Lan S., Stobart R., Chen R., Performance comparison of a thermoelectric generator applied in conventional vehicles and extended-range electric vehicles, *Energy Conversion and Management*, **266**: 115791, 2022, https://doi.org/10.1016/j.enconman.2022.115791.
8. Zhang Q., Wang L.J., Li G., Liu Y., A real-time energy management control strategy for battery and supercapacitor hybrid energy storage systems of pure electric vehicles, *Journal of Energy Storage*, **31**: 101721, 2020, https://doi.org/10.1016/j.est.2020.101721.
9. Kopczyński A., Liu Z., Krawczyk P., Parametric analysis of Li-ion battery based on laboratory tests, *E3S Web Conference*, **44**: 00074, 2018, https://doi.org/10.1051/e3sconf/20184400074.
10. Li W., Cui H., Nemeth T., Jansen J., Ünlübayir C., Wei Z., Zhang L., Wang Z., Ruan J., Dai H., Wei X., Sauer D.U., Deep reinforcement learning-based energy management of hybrid battery systems in electric vehicles, *Journal of Energy Storage*, **36**: 102355, 2021, https://doi.org/10.1016/j.est.2021.102355.

11. Du J.Y., Chen J.F., Song Z.Y., Gao M.M., Ouyang M.G., Design method of a power management strategy for variable battery capacities range-extended electric vehicles to improve energy efficiency and cost-effectiveness, *Energy*, **121**: 32–42, 2017, https://doi.org/10.1016/j.energy.2016.12.120.

12. Li J.Q., Jin X., Xiong R., Multi-objective optimization study of energy management strategy and economic analysis for a range-extended electric bus, *Applied Energy*, **194**: 798–807, 2017, https://doi.org/10.1016/j.apenergy.2016.10.065.

13. Li J.Q., Wang Y.H., Chen J.W., Zhang X.P., Study on energy management strategy and dynamic modeling for auxiliary power units in range-extended electric vehicles, *Applied Energy*, **194**: 363–375, 2017, https://doi.org/10.1016/j.apenergy.2016.09.001.

14. Lasocki J., Krawczyk P., Kopczyński A., Roszczyk P., Hajduga A., Analysis of the strategies for managing extended-range electric vehicle powertrain in the urban driving cycle, *Electrical Engineering & Electromechanics*, **2022**(1): 70–76, 2022, https://doi.org/10.20998/2074-272X.2022.1.10.

15. Krawczyk P., Kopczyński A., Lasocki J., Modeling and simulation of extended-range electric vehicle with control strategy to assess fuel consumption and CO_2 emission for the expected driving range, *Energies*, **15**(12): 4187, 2022, https://doi.org/10.3390/en15124187.

16. Di Ilio G., Bella G., Jannelli E., Performance evaluation of extended-range electric vehicles equipped with hydrogen-fueled rotary engine, *SAE Technical Paper*, 2020-24-0011, 2020, https://doi.org/10.4271/2020-24-0011.

17. Jiang Y., Zhang Y., Zhang B., Chen Y., Study on methanol-hydrogen engine in extended-range electric vehicles, *International Journal of Engine Research*, **25**(6): 1136–1145, 2024, https://doi.org/10.1177/14680874231220532.

18. Barakat A.A., Diab J.H., Badawi N.S., Bou Nader W.S., Mansour C.J., Combined cycle gas turbine system optimization for extended range electric vehicles, *Energy Conversion and Management*, **226**: 113538, 2020, https://doi.org/10.1016/j.enconman.2020.113538.

19. Kopczyński A., Krawczyk P., Lasocki J., Parameters selection of extended-range electric vehicle supplied with alternative fuel, *E3S Web Conference*, **44**: 00073, 2018, https://doi.org/10.1051/e3sconf/20184400073.

20. Lasocki J., Kopczyński A., Krawczyk P., Roszczyk P., Empirical study on the efficiency of an LPG-supplied range extender for electric vehicles, *Energies*, **12**: 18, 2019, https://doi.org/10.3390/en12183528.

21. Duc K.N., Duy V.N., Study on performance enhancement and emission reduction of used fuel-injected motorcycles using bi-fuel gasoline-LPG, *Energy for Sustainable Development*, **43**: 60–67, 2018, https://doi.org/10.1016/j.esd.2017.12.005.

22. Baczewski K., Kałdoński T., *Fuels for Spark-Ignition Engines* [in Polish: *Paliwa do silników o zapłonie iskrowym*], WKŁ, Warszawa 2005.

Received December 19, 2024; accepted version June 10, 2025.
Online first August 5, 2025.